

On the anomalous large-scale flows in the Universe

Davor Palle

Zavod za teorijsku fiziku, Institut Rugjer Bošković
Bijenička cesta 54, 10002 Zagreb, Croatia

Revised: 19 June 2010

Abstract. Recent combined analyses of the CMB and galaxy cluster data reveal unexpectedly large and anisotropic peculiar velocity fields at large scales. We study cosmic models with included vorticity, acceleration and total angular momentum of the Universe in order to understand the phenomenon. The Zel'dovich model is used to mimic the low redshift evolution of the angular momentum. Solving coupled evolution equations of the second order for density contrast in corrected Ellis-Bruni covariant and gauge-invariant formalism one can properly normalize and evaluate integrated Sachs-Wolfe effect and peculiar velocity field. The theoretical results compared to the observations favor a much larger matter content of the Universe than that of the concordance model. Large-scale flows appear anisotropic with dominant components placed in the plane perpendicular to the axis of vorticity (rotation). The integrated Sachs-Wolfe term has a negative contribution to the CMB fluctuations for the negative cosmological constant and it can explain the observed small power of the CMB TT spectrum at large scales. The rate of the expansion of the Universe may be substantially affected by the angular momentum if its magnitude is large enough.

PACS. PACS-98.80.Es Observational cosmology(including Hubble constant, distance scale, cosmological constant, early Universe, etc.) – PACS-12.10.Dm Unified theories and models of strong and electroweak interactions – PACS-04.60.-m Quantum gravity

1 Introduction and motivation

Modern cosmology relies heavily on two paradigms in order to fit vast astrophysical datasets: 1. the existence of dark matter and 2. the existence of dark energy. It is assumed that dark matter consists of the neutral weakly interacting fermion decoupled from primordial plasma as a nonrelativistic species (cold dark matter=CDM). The CDM-mass-density behavior on redshift is the standard one of nonrelativistic matter. The origin and the redshift behavior of dark energy is rather obscure. The concordance Λ CDM model presumes that dark energy is positive cosmological constant.

Dark matter is thus a problem of particle physics, while dark energy is a common problem of field theory, particle physics and the theory of gravity.

The common mathematical difficulties of the zero distance singularity and causality motivate the proposal for a new symmetry-breaking mechanism in particle physics (BY theory of ref. [1]) and new studies in the Einstein-Cartan theory of gravity. Heavy Majorana neutrinos within the nonsingular and causal SU(3) electroweak-strong unification [1] represent the main building block of the Universe as a cold dark matter (DM) particles. They are cosmologically stable $\tau_{N_i} \gg \tau_U$ with large annihilation cross sections [2]. The H.E.S.S. source J1745-290 [3] in the center of our galaxy and WMAP haze [4] are possible indications of the heavy DM particle annihilations.

Light Majorana neutrinos trigger vorticity of the Universe [5,6] through the spin-torsion relations in the Einstein-Cartan cosmology at early times of the evolution. The formation of large-scale structures in the form of galaxies and clusters, as well as, the present anisotropy of spacetime, not predicted by inflation of the concordance Λ CDM model, indicate the existence of nonvanishing total angular momentum of the Universe.

The current measurements of the CMB by WMAP, the large catalogues of SDSS, the new cluster and the peculiar velocity catalogues motivate us to undertake considerations to explain features that are not expected in the concordance Λ CDM model-anisotropic anomalous large-scale flows. The low power of large-scale TT CMB fluctuations observed by COBE and WMAP, discrepant with the Λ CDM model, should be explained with new cosmologies.

In the next chapter we derive the evolution equations of density contrast for models with expansion, vorticity, acceleration and angular momentum within the corrected Ellis-Bruni formalism. A comparison is made with the standard formulas of isotropic and homogeneous spacetime. One can then evaluate integrated Sachs-Wolfe effect and RMS peculiar velocity field for any model.

The last chapter is devoted for discussions, conclusions and suggestions for future work. Appendices contain detailed framework for Einstein-Cartan cosmology with field equations, propagation equations and a comparison of the corrected and standard Ellis-Bruni fluid-flow approach for the density-contrast evolution.

2 Evolution equations

Our interest is the evolution of the Universe during the matter dominated epoch. The standard lore for the evolution of the density contrast, peculiar acceleration and peculiar velocity field gives the following equations [7, 8, 9]:

$$\delta(a, \mathbf{k}) \equiv \delta(a)\delta_{\mathbf{k}}, \quad \delta(\mathbf{x}) = \int d^3k e^{i\mathbf{k}\cdot\mathbf{x}} \delta_{\mathbf{k}},$$

$$\mathbf{v}_{\mathbf{k}} = \frac{i\mathbf{k}}{k^2} a \dot{a} \delta_{\mathbf{k}} \frac{d\delta(a)}{da}, \quad a = R(t)/R_0 = 1/(1+z). \quad (1)$$

The root mean square (RMS) values of the mass-density contrast and the peculiar velocity field at a certain scale S and the redshift z using Gaussian window functions [7, 8, 9] are defined as:

$$(\delta M/M)_{RMS}^2(a, S) \equiv \langle (\delta M/M)^2 \rangle(a, S) = NV_W^{-2} \int d^3k W^2(\mathbf{k}, S) \delta^2(a) |\delta_{\mathbf{k}}|^2, \quad (2)$$

$$v_{RMS}^2(a, S) \equiv \langle v^2 \rangle(a, S) = NV_W^{-2} \int d^3k W^2(\mathbf{k}, S) \frac{1}{k^2} (a \dot{a} \frac{d\delta(a)}{da})^2 |\delta_{\mathbf{k}}|^2, \quad (3)$$

$$V_W = \frac{4\pi}{3} S^3, \quad W(\mathbf{k}, S) = (2\pi)^{3/2} S^3 e^{-\frac{1}{2} S^2 \mathbf{k}^2}.$$

The aim is to study cosmological models with vorticity, acceleration and nonvanishing total angular momentum through torsion effects. We use the standard CDM power spectrum $P(k) = |\delta_{\mathbf{k}}|^2$ defined in [8].

The growth function $\delta(a)$ must be studied carefully. Our choice of covariant spacelike vectors within a fluid-flow formalism differs from that of Ellis and Bruni [10]:

$$\delta = (-\mathcal{D}_\mu \mathcal{D}^\mu)^{1/2}, \quad \mathcal{D}_\mu \equiv R^2(t) \rho^{-1} h_\mu^\nu \tilde{\nabla}_\nu \rho, \quad (4)$$

$$\mathcal{L}_\mu \equiv R^2(t) h_\mu^\nu \tilde{\nabla}_\nu \Theta.$$

These vectors fulfil the Stewart-Walker lemma [11] and their evolution equations result in a correct solution for a density contrast formed from their scalar invariants. This is not the case for the standard Ellis-Bruni covariant vectors.

The detailed derivation of the equations one can find in Appendix A while a comparison between two fluid-flow approaches is in Appendix B.

The resulting second order coupled equations in our corrected scheme are given by (matter dominated regime):

$$\begin{aligned} & \ddot{\mathcal{D}}_\mu - \frac{1}{3} \dot{\Theta} \mathcal{D}_\mu - \frac{1}{3} \Theta \dot{\mathcal{D}}_\mu + a_\mu a^\nu \mathcal{D}_\nu + u_\mu \dot{a}^\nu \mathcal{D}_\nu + u_\mu a^\nu \dot{\mathcal{D}}_\nu \\ & - \left(\frac{1}{3} \Theta \delta_\mu^\lambda + u_\mu a^\lambda + \tilde{\omega}_{\cdot\mu}^\lambda + \sigma_{\cdot\mu}^\lambda \right) \left(\frac{1}{3} \Theta \mathcal{D}_\lambda - u_\lambda a^\nu \mathcal{D}_\nu - \dot{\mathcal{D}}_\lambda - \mathcal{D}_\rho (\sigma_{\cdot\lambda}^\rho + \tilde{\omega}_{\cdot\lambda}^\rho) + \Theta R^2 a_\lambda \right) \\ & - 2a_\mu R^2 \dot{\Theta} - R^2 {}^{(3)}\tilde{\nabla}_\mu \mathcal{N} - \frac{1}{2} \kappa \rho \mathcal{D}_\mu + \dot{\mathcal{D}}_\lambda (\sigma_{\cdot\mu}^\lambda + \tilde{\omega}_{\cdot\mu}^\lambda) \\ & + \mathcal{D}_\lambda (\dot{\sigma}_{\cdot\mu}^\lambda + \dot{\tilde{\omega}}_{\cdot\mu}^\lambda) - \frac{2}{3} R^2 \Theta^2 a_\mu - \Theta R^2 \dot{a}_\mu = 0, \end{aligned} \quad (5)$$

$$\mathcal{N} = 2\sigma^2 - 2\tilde{\omega}^2 - \tilde{\nabla}_\mu a^\mu.$$

We use the Zel'dovich model to describe the evolution of the total angular momentum of the Universe at small redshifts [9] assuming the surplus of right-handed over left-handed galaxies and clusters [6, 12]

$$\begin{aligned}
\mathbf{L}(t) &\propto a^2 \dot{a} \bar{\rho} \int_{V_L} d^3q (\mathbf{q} - \bar{\mathbf{q}}) \times [\nabla \Phi_0(q) - \nabla \Phi_0(\bar{q})], \\
\mathbf{L}(\text{Universe}) &\propto [n(\text{right}) - n(\text{left})] \mathbf{L}(t), \\
Q = \text{torsion} &\propto L(\text{Universe}) \Rightarrow Q(a) = Q_0 a^{-3/2} \text{ for } z = a^{-1} - 1 < z_{cr} = 4, \\
&\text{where } z_{cr} = 4 \text{ is put arbitrarily, otherwise } Q(z > z_{cr}) = 0.
\end{aligned} \tag{6}$$

The Einstein-Cartan equations remain unaltered with respect to the functional form of the time dependence of torsion (see Appendix A).

We have to factorize density contrast on the space and time dependent parts. One can achieve this goal transforming the evolution equations for covariant vectors to the local Lorentzian frame by tetrads:

$$\mathcal{D}_a = v_a^\mu \mathcal{D}_\mu, \quad g^{\mu\nu} = v_a^\mu v_b^\nu \eta^{ab}, \quad \delta = (-\mathcal{D}_a \mathcal{D}^a)^{1/2},$$

$$\eta^{ab} = \text{diag}(+1, -1, -1, -1), \quad \mu, \nu = 0, 1, 2, 3, \quad a, b = \hat{0}, \hat{1}, \hat{2}, \hat{3}.$$

In the Appendix A one can find evaluated coefficients for the following spacetime metric:

$$\begin{aligned}
ds^2 &= dt^2 - R^2(t)[dx^2 + (1 - \lambda^2(t))e^{2mx} dy^2] - R^2(t)dz^2 - 2R(t)\lambda(t)e^{mx} dydt, \\
& \quad m = \text{const.}
\end{aligned} \tag{7}$$

It is easy to verify that in the Friedmann limit one recovers the standard form of the density contrast [13] (see Appendix A):

$$\begin{aligned}
\delta(a) &= \frac{H(a)}{H_0} \int_0^a da a^{-3} \left[\frac{H_0}{H(a)} \right]^3, \\
H(a) &= H_0 (\Omega_m a^{-3} + \Omega_\Lambda)^{1/2}.
\end{aligned} \tag{8}$$

One can evaluate properly normalized peculiar velocities and integrated Sachs-Wolfe effect for various cosmological models [13]:

$$\begin{aligned}
a_{lm}^{ISW} &= 12\pi i^l \int d^3k Y_l^{m*}(\hat{k}) \delta_{\mathbf{k}} \left(\frac{H_0}{k} \right)^2 \int da j_l(kr) \chi^{ISW}, \\
\chi^{ISW} &= -\Omega_m \frac{d}{da} (\delta(a)/a), \quad r = \int_a^1 da a^{-2} H^{-1}(a), \quad \delta(a=1) = 1.
\end{aligned} \tag{9}$$

3 Results and discussion

Supplied with all the necessary equations we can evaluate properly normalized peculiar velocities and integrated Sachs-Wolfe effect. We use the same normalization for all cosmological models:

$$(\delta M/M)_{RMS}(a=1, S=10h^{-1} \text{Mpc}) = 1.$$

This is the standard normalization suitable for the study of peculiar velocities (see p.262 of ref.[9]). We aim to compare cosmic models with respect to the concordance Λ CDM model, not to perform a precision fit to data.

Let us fix relevant parameters of the models in Table I (unit $H_0 = 1$ is used for parameters m , λ_0 and Q_0 ; EdS=Einstein-de Sitter, EC=Einstein-Cartan, Λ CDM=concordance model, $\Omega_\Lambda = 1 - \Omega_m$, $\lambda = \lambda_0 R^{-1}$, $Q = Q_0 R^{-3/2}$, $R_0 = H_0^{-1}$).

The formation of small-scale structures and the age of the Universe can be explained with a larger mass-density and smaller Hubble constant (see Table II). This statement is valid if we assume that the total angular momentum of the Universe at low redshifts, acting through torsion terms, is much smaller than mass-density terms. The evolution with large torsion terms must contain feedback from matter to the background geometry, changing substantially its

Table 1. Model parameters

	Ω_m	h	m	λ_0	Q_0
Λ CDM	0.3	0.7	0	0	0
EdS	1	0.5	0	0	0
EC1	2	0.4	0.03	0.067	-0.2
EC2	2	0.4	0	0	0
EC3	2	0.4	0.3	0.67	0

Table 2. Age of the Universe

	Λ CDM	EdS	EC1	EC2
τ_U (Gyr)	13.77	13.33	13.14	13.09

Table 3. v_{rms} (km/s) for the Λ CDM model

z \ S(Mpc)	50	187.5	325	462.5	600
0	511.67	184.73	111.75	79.95	62.21
0.25	515.49	186.11	112.58	80.55	62.67
1	467.16	168.66	102.03	73.00	56.80

Table 4. v_{rms} (km/s) for the EdS model

z \ S(Mpc)	50	187.5	325	462.5	600
0	766.27	245.82	145.55	103.27	80.00
0.25	685.38	218.87	130.18	92.37	71.56
1	541.84	173.82	102.92	73.03	56.57

Table 5. v_{rms} (km/s) for the EC1 model

z \ S(Mpc)	50	187.5	325	462.5	600
0	1090.94	335.81	197.54	139.83	108.19
0.25	901.75	277.58	163.28	115.58	89.42
1	678.04	208.71	122.78	86.91	67.24

Table 6. v_{rms} (km/s) for the EC2 model

z \ S(Mpc)	50	187.5	325	462.5	600
0	1091.69	336.04	197.68	139.92	108.26
0.25	902.28	277.74	163.38	115.65	89.48
1	678.45	208.84	122.85	86.96	67.28

expansion and vorticity. It is possible to utilize this approach within N-body simulations. Thus, we limit numerical evaluations in this paper to small torsion contributions.

From Tables III-VI it is clear that only models with large mass-density can enhance large-scale peculiar velocities observed in the analyses with combined cluster and WMAP data [14,15,16]. Rather small amounts of vorticity, acceleration or torsion do not essentially influence RMS velocities. However, components of a density contrast \mathcal{D}_i , $i = 1, 2, 3$ are not equal. We assume the standard scaling of the vorticity [7]: $\lambda(a) = \lambda_0 a^{-1} \Rightarrow \omega \propto a^{-2}$ (see Appendix for definitions).

The density contrasts normalized at zero-redshift do not depend on the initial cosmic scale factor, but a difference between components does depend. One can estimate the resulting angle between the axis of vorticity (z-axis) and the anisotropic bulk velocity. The angle depends on the initial redshift and the magnitude of the vorticity ($\omega(t) = \frac{1}{2}m\lambda(t)R(t)^{-1}$):

$$a(initial) = 10^{-2}, a(final) = 1, model = EC1, \frac{\omega_0}{H_0} = \frac{1}{2}m\lambda_0 = 10^{-3}$$

$$\Rightarrow \angle(\hat{n}(flow), \hat{n}(axis)) = \arctg \frac{(\mathcal{D}_1^2 + \mathcal{D}_2^2)^{1/2}}{|\mathcal{D}_3|} = 55.3^\circ,$$

$$a(initial) = 10^{-2}, a(final) = 1, model = EC1, but m = 0.15: \angle(\hat{n}(flow), \hat{n}(axis)) = 57.25^\circ,$$

$$a(initial) = 10^{-3}, a(final) = 1, model = EC1: \angle(\hat{n}(flow), \hat{n}(axis)) = 72.3^\circ.$$

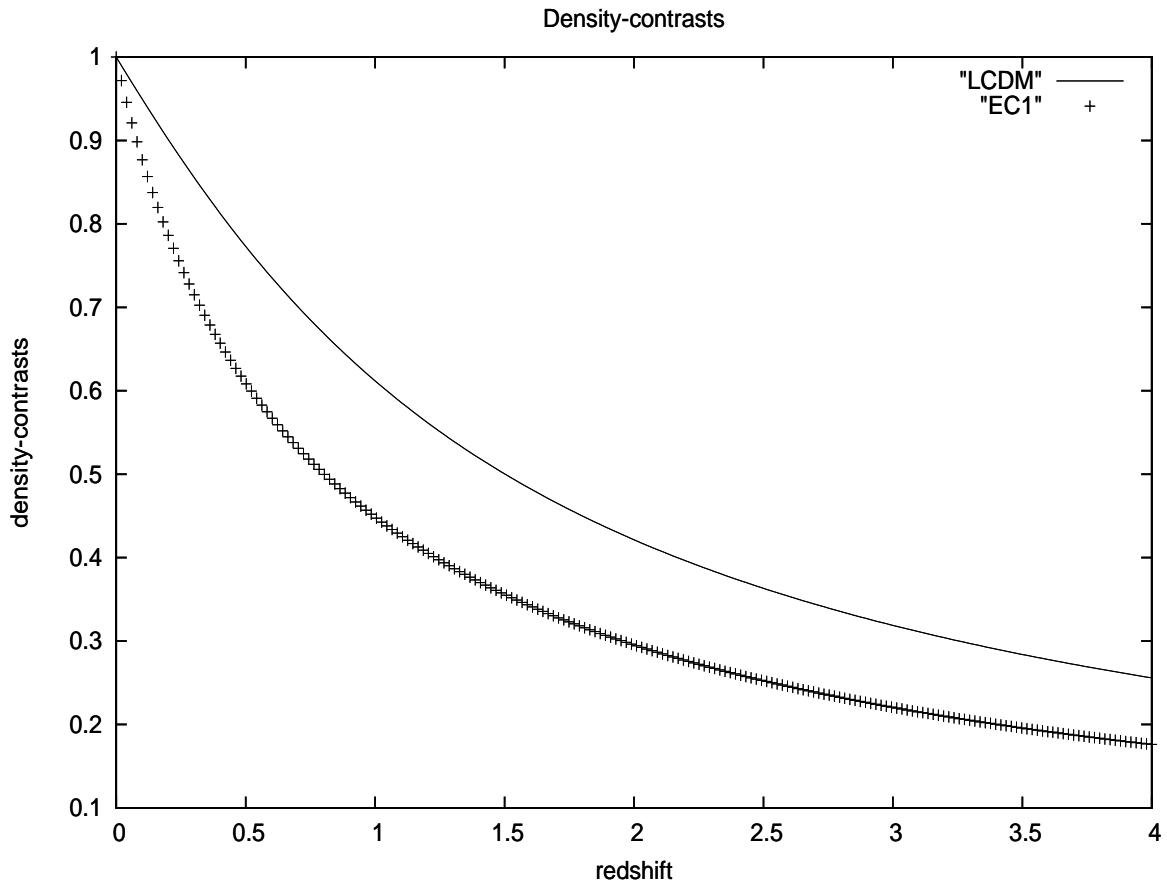


Fig. 1. Density contrasts for the Λ CDM and EC1 models.

Since the metric describes rotation around z-axis, the dominant components of over(under)densities, the peculiar accelerations and the velocities are placed in the plain perpendicular to the axis of rotation (vorticity). We estimate the angle between the measured directions of the axis of vorticity [17] and the large-scale flows [15]:

$$\begin{aligned} \hat{n}(flow) &= (l = 287^\circ, b = 8^\circ), \quad \hat{n}(axis) = (l = 260^\circ, b = 60^\circ) \\ &\Rightarrow \angle(\hat{n}(flow), \hat{n}(axis)) = 53^\circ. \end{aligned}$$

The reader can compare and visualize density contrasts and their derivatives for two crucial models (Λ CDM and EC) in Figs. 1 and 2.

The integrated Sachs-Wolfe effect is negative for large mass-density models (EC) with negative cosmological constant, while it is positive for Λ CDM, as can be seen in Fig. 3. The negative contribution of the ISW decreases the total amplitude of the CMB fluctuation, while the positive ISW of the Λ CDM increases it [18]. The observations point to very small power at large scales, in contradiction with the Λ CDM model.

It seems that the introduction of rotational degrees of freedom (torsion, spin, vorticity, angular momentum) is inevitable in order to understand and fit all observational data. Two scenarios emerge as viable resolutions: (1) small Hubble constant with small amount of the total angular momentum of the Universe at present or possibly: (2) larger Hubble constant if the total angular momentum appears much larger. Torsion terms (linear and quadratic) always give a negative contribution to the effective mass-density, as it can be seen from Einstein-Cartan field equations (see Appendix A).

Recent measurements of the Hubble constant [19] give a large value, thus EC1 type models with small contribution of torsion (angular momentum) at low redshifts are ruled out. The concordance model cannot accommodate to the low power of density fluctuations at large scales because of the positive contribution of the ISW effect for the positive cosmological constant. It has unsurmountable difficulties to explain large peculiar velocities, while the observed anisotropies of the CMB fluctuations and peculiar velocities are complete surprise for the astrophysical community violating fundamental cosmological principle of the isotropic Universe.

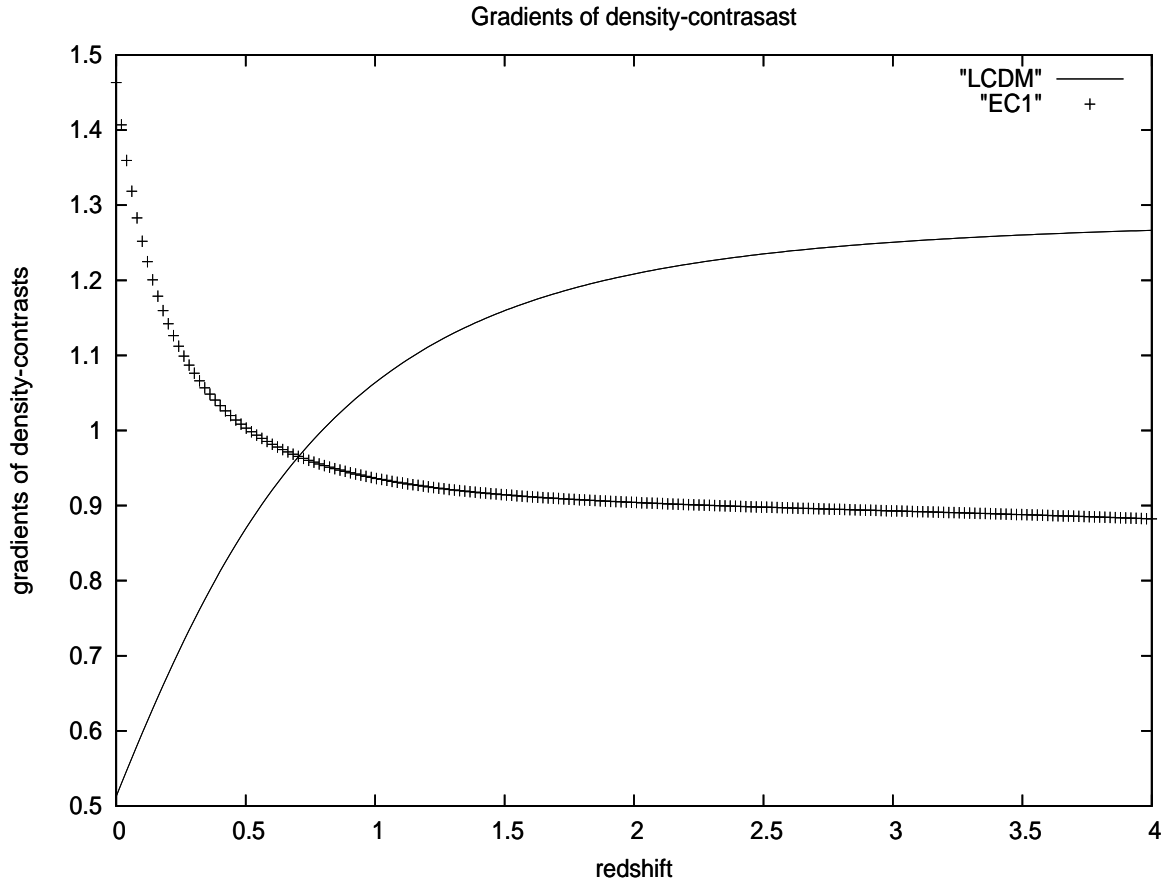


Fig. 2. Gradients of the density contrasts $\frac{d\delta}{da}$ for the Λ CDM and EC1 models.

Let us briefly comment some results of the analyses of cluster data by various projects and groups. Some groups conclude that the mass density of the Universe is low like in the concordance model [20], while other groups draw a conclusion for a large mass density [21]. Large uncertainty in the L-T relations is a probable cause of the discrepant conclusions.

There is a general belief that the CMB measurements are the most reliable tool to constrain cosmic parameters. One cannot ignore disturbing objections for possibly erroneous analyses of time ordered data [22] or problems with beam profile sensitivity [23] in WMAP papers. Any error can affect the estimate of cosmic parameters.

The equation of state for dark energy is a target of an extensive research by supernovae [24] or by combined data [25]. Even tests of the concordance model by studying local group dynamics provoke more questions than answers [26]. It should be mentioned that the unusual time dilation in quasar light curves [27] should be eventually explained by lensing within different cosmic models.

The second scenario with large torsion content at low redshifts is the most plausible model capable to surmount difficulties of the concordance model and EC1 type models. From the work in ref.[5] one can conclude that $\lim_{R \rightarrow \infty} \rho_M / \rho_\Lambda = -2$, but $\lim_{R \rightarrow \infty} \rho_M = 0$ and then $\rho_\Lambda = 0$. It follows that the torsion contribution plays a role of the negative dark energy (see [5] and Eq.(16)) $\rho_{M,0} / \rho_{torsion,0} \simeq -2$, making possible the introduction of the large Hubble parameter necessary for more accurate cosmic clocks and the age of the Universe (see Eq.(17)). Considerations with large angular momentum (torsion) of the Universe must include N-body numerical simulations. Dark energy, described by a torsion, should be a clustered physical quantity [28] dependent on redshift [29].

To conclude, it is of great importance to search for an independent method to fix ρ_M , not only the total density ρ_{tot} . The idea of Zwicky [30] to study galaxy and cluster catalogues (SDSS etc.) to estimate directly the mass density of matter could be advantageous.

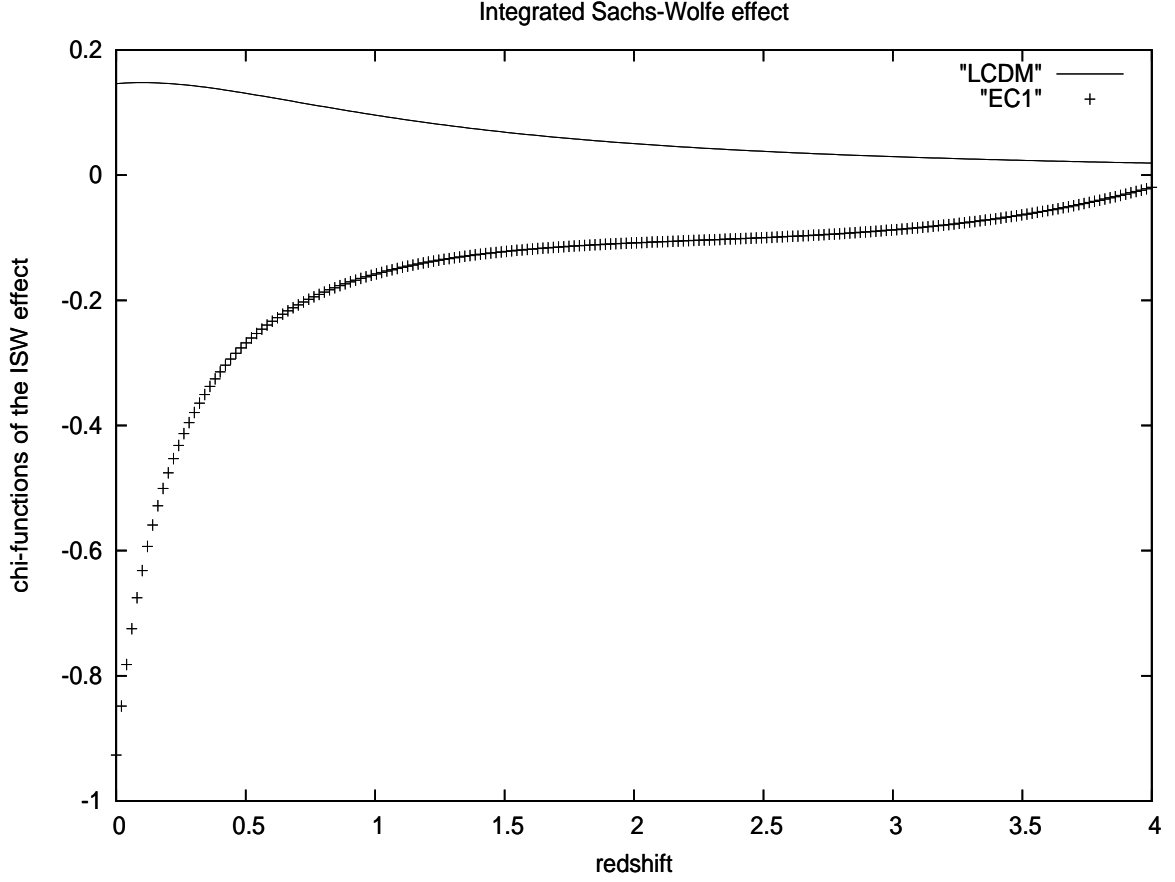


Fig. 3. Integrated Sachs-Wolfe χ^{ISW} function for the Λ CDM and EC1 models.

4 Appendix A

We provide here a complete set of conventions, identities and equations for Einstein-Cartan theory. $g_{\mu\nu}$ is a metric tensor defined in Eq.(7), $R(t)$ is a cosmic scale factor, $\lambda(t)$ function is proportional to the acceleration vector a_μ in Eq.(11), m parameter of $g_{\mu\nu}$ defines vorticity in Eq.(11), $Q^\alpha_{\beta\gamma}$ is a torsion tensor, $S^\alpha_{\beta\gamma}$ is a spin tensor, v_a^μ are tetrad fields, ρ denotes mass density, p denotes pressure of the fluid, Λ is a cosmological constant, u_μ is a velocity four-vector, $Q^2 = 1/2Q_{\mu\nu}Q^{\mu\nu}$, $Q^\alpha_{\cdot\mu\nu} = u^\alpha Q_{\mu\nu}$, $a = R(t)/R_0$ in Eq.(17) is a dimensionless cosmic scale factor, h in Eq.(17) is a Hubble parameter, A in Eq.(18) is a normalization constant.

The metric is defined as:

$$g^{\mu\nu} = v_a^\mu v_b^\nu \eta^{ab}, \quad \eta_{ab} = \text{diag}(+1, -1, -1, -1),$$

$$\mu, \nu = 0, 1, 2, 3, \quad a, b = \hat{0}, \hat{1}, \hat{2}, \hat{3},$$

$$\tilde{\Gamma}^\alpha_{\beta\mu} = \Gamma^\alpha_{\beta\mu} + Q^\alpha_{\cdot\beta\mu} + Q_{\beta\mu}^{\cdot\alpha} + Q_{\beta\mu}^{\cdot\alpha},$$

$$\tilde{R}^\lambda_{\cdot\sigma\mu\nu} = \partial_\mu \tilde{\Gamma}^\lambda_{\sigma\nu} - \partial_\nu \tilde{\Gamma}^\lambda_{\sigma\mu} + \tilde{\Gamma}^\lambda_{\beta\mu} \tilde{\Gamma}^\beta_{\sigma\nu} - \tilde{\Gamma}^\lambda_{\beta\nu} \tilde{\Gamma}^\beta_{\sigma\mu}.$$

Field equations and Ricci identities look thus [31]:

$$\tilde{R}_{\mu\nu} - \frac{1}{2}g_{\mu\nu}\tilde{R} = \kappa\tilde{T}_{\mu\nu}, \quad \tilde{R}_{\mu\nu} = \tilde{R}^\lambda_{\cdot\mu\lambda\nu}, \quad \tilde{R} = \tilde{R}^\mu_{\cdot\mu},$$

$$Q^\mu_{\cdot ab} + 2v_a^\mu Q_b] = \kappa S^\mu_{\cdot ab}, \quad \kappa = 8\pi G_N c^{-4},$$

$$Q_a = v_a^\mu Q_\mu, \quad Q_\mu = Q^\mu_{\cdot\mu}, \quad [ab] = 1/2(ab - ba), \quad (ab) = 1/2(ab + ba)$$

$$\begin{aligned} (\tilde{\nabla}_\mu \tilde{\nabla}_\nu - \tilde{\nabla}_\nu \tilde{\nabla}_\mu) u_\lambda &= -\tilde{R}^\sigma_{\lambda\mu\nu} u_\sigma - 2Q^\sigma_{\nu\mu} \tilde{\nabla}_\sigma u_\lambda, \\ \tilde{\nabla}_\alpha u_\beta &= \partial_\alpha u_\beta - \tilde{\Gamma}^\nu_{\beta\alpha} u_\nu. \end{aligned}$$

Conformal or Weyl tensor $\tilde{C}_{\sigma\lambda\mu\nu}$ is defined as:

$$\begin{aligned} \tilde{R}_{\sigma\lambda\mu\nu} &= \frac{1}{2}(g_{\sigma\mu}\tilde{R}_{\lambda\nu} - g_{\sigma\nu}\tilde{R}_{\lambda\mu} - g_{\lambda\mu}\tilde{R}_{\sigma\nu} + g_{\lambda\nu}\tilde{R}_{\sigma\mu}) \\ &\quad - \frac{1}{6}\tilde{R}(g_{\sigma\mu}g_{\lambda\nu} - g_{\sigma\nu}g_{\lambda\mu}) + \tilde{C}_{\sigma\lambda\mu\nu}. \end{aligned}$$

The energy-momentum tensor of the Weyssenhoff fluid is derived by Obukhov and Korotky [32]:

$$T_{\mu\nu} = -(p - \Lambda)g_{\mu\nu} + u_\mu[u_\nu(\rho + p) + 2u^\alpha \tilde{\nabla}_\beta S^\beta_{\alpha\nu}]. \quad (10)$$

The Ehlers-decomposition of the velocity-gradient can be written as

$$\begin{aligned} \tilde{\nabla}_\mu u_\nu &= \tilde{\omega}_{\nu\mu} + \sigma_{\mu\nu} + \frac{1}{3}\Theta h_{\mu\nu} + u_\mu a_\nu, \\ u^\mu u_\mu &= 1, \quad h_{\mu\nu} = g_{\mu\nu} - u_\mu u_\nu, \quad a_\mu = u^\nu \tilde{\nabla}_\nu u_\mu, \quad \Theta = \tilde{\nabla}_\nu u^\nu, \\ \tilde{\omega}_{\mu\nu} &= h_\mu^\alpha h_\nu^\beta \tilde{\nabla}_{[\beta} u_{\alpha]}, \quad \sigma_{\mu\nu} = h_\mu^\alpha h_\nu^\beta \tilde{\nabla}_{(\alpha} u_{\beta)} - \frac{1}{3}\Theta h_{\mu\nu}. \end{aligned} \quad (11)$$

The vorticity is uniquely defined by a variational principle (see Eq. (3.11) of [32]):

$$\tilde{\omega}_{ij} = v_i^\mu (\tilde{\nabla}_\alpha v_j^\nu) u^\alpha g_{\mu\nu}, \quad i, j = \hat{1}, \hat{2}, \hat{3}. \quad (12)$$

The above two formulas for vorticity agree, but a formula for vorticity in (5.5) of [32] has a wrong sign, as well as definitions of vorticity in [33] and [34]. Eventually, this confusion caused some wrong terms in the derivation of the evolution equations in [35], as it is pointed out in [34] and later in [36].

The standard procedure leads to the evolution equations (Frenkel condition employed $u^\mu Q_{,\mu\nu}^\kappa = 0$):

$$\begin{aligned} \dot{F} &\equiv u^\mu \tilde{\nabla}_\mu F, \quad \tilde{\omega}^2 = \frac{1}{2}\tilde{\omega}_{\mu\nu}\tilde{\omega}^{\mu\nu}, \quad \sigma^2 = \frac{1}{2}\sigma_{\mu\nu}\sigma^{\mu\nu}, \\ \dot{\Theta} &= \tilde{\nabla}_\mu a^\mu + 2\tilde{\omega}^2 - 2\sigma^2 - \frac{1}{3}\Theta^2 - \tilde{R}_{\sigma\nu} u^\sigma u^\nu, \\ h_\alpha^{[\nu} h_\beta^{\lambda]} \dot{\tilde{\omega}}_{\nu\lambda} &= -\frac{2}{3}\Theta \tilde{\omega}_{\alpha\beta} - 2\sigma_{[\alpha}^\gamma \tilde{\omega}_{\gamma|\beta]} - h_\alpha^{[\nu} h_\beta^{\lambda]} \tilde{\nabla}_\nu a_\lambda + h_\alpha^{[\nu} h_\beta^{\lambda]} u^\mu u^\kappa \tilde{R}_{\kappa\lambda\mu\nu}, \\ h_\nu^\alpha h_\mu^\beta \dot{\sigma}_{\alpha\beta} &= h_\nu^\alpha h_\mu^\beta \tilde{\nabla}_{(\alpha} a_{\beta)} - a_\nu a_\mu - \tilde{\omega}_{(\nu|\rho} \tilde{\omega}^{\rho}_{|\mu)} - \sigma_{\nu\alpha} \sigma_\mu^\alpha \\ &\quad - \frac{2}{3}\Theta \sigma_{\nu\mu} - \frac{1}{3}h_{\nu\mu}[2(\tilde{\omega}^2 - \sigma^2) + \tilde{\nabla}_\alpha a^\alpha] - E_{(\nu\mu)}, \\ E_{\alpha\beta} &= \tilde{C}_{\sigma\alpha\mu\beta} u^\sigma u^\mu. \end{aligned}$$

We use the following identity:

$${}^{(3)}\tilde{\nabla}_\mu(\dot{f}) - h_\mu^\nu ({}^{(3)}\tilde{\nabla}_\nu f)^\cdot = a_\mu \dot{f} + (\tilde{\omega}_{,\mu}^\lambda + \sigma_{\mu,\lambda}^\lambda + \frac{1}{3}\Theta h_\mu^\lambda) ({}^{(3)}\tilde{\nabla}_\lambda f), \quad (13)$$

and the continuity equation in matter dominated epoch:

$$u^\mu \tilde{\nabla}_\mu \rho + \rho \tilde{\nabla}_\mu u^\mu = 0 \quad (14)$$

to derive the evolution equation for density contrast Eq.(5).

We evaluate the coefficients of the coupled evolution equations for components in the local Lorentzian frame \mathcal{D}_a with the metric of Eq.(7) (time component \mathcal{D}_0 can be set to zero because of the relation $u^a \mathcal{D}_a = 0$):

$$\ddot{\mathcal{D}}_i + b_{ij} \dot{\mathcal{D}}_j + a_{ik} \mathcal{D}_k + d_i = 0, \quad i, j, k = 1, 2, 3, \quad (15)$$

$$\begin{aligned} a_{11} = & -\frac{1}{3}\dot{\lambda}^2 - \frac{1}{3}\kappa\Lambda - \frac{5}{3}Q^2 - \frac{1}{3}\kappa\rho - \frac{5}{3}\frac{\dot{R}}{R}\lambda\dot{\lambda} \\ & - \frac{1}{3}\ddot{\lambda}\lambda + \frac{5}{3}\frac{m}{R}\lambda Q - \frac{2}{3}\lambda^2\frac{\dot{R}^2}{R^2} - \frac{5}{12}\left(\lambda\frac{m}{R}\right)^2 - \frac{1}{3}\frac{\ddot{R}}{R}(-3 + \lambda^2), \end{aligned}$$

$$a_{12} = \frac{1}{2}\frac{m}{R}\dot{\lambda} + \frac{1}{4}\frac{\dot{R}}{R}Q + \frac{1}{2}\lambda\frac{m}{R}\frac{\dot{R}}{R}, \quad a_{13} = 0,$$

$$b_{11} = 2\frac{\dot{R}}{R}, \quad b_{12} = -2Q + \lambda\frac{m}{R}, \quad b_{13} = 0,$$

$$a_{21} = -\frac{1}{2}\frac{m}{R}\dot{\lambda} - \frac{1}{4}\frac{\dot{R}}{R}Q - \frac{1}{2}\lambda\frac{m}{R}\frac{\dot{R}}{R},$$

$$\begin{aligned} a_{22} = & -\frac{4}{3}\dot{\lambda}^2 - \frac{1}{3}\kappa\Lambda - \frac{5}{3}Q^2 - \frac{1}{3}\kappa\rho - \frac{11}{3}\frac{\dot{R}}{R}\lambda\dot{\lambda} \\ & - \frac{1}{3}\ddot{\lambda}\lambda + \frac{5}{3}\frac{m}{R}Q\lambda - \frac{5}{3}\lambda^2\left(\frac{\dot{R}}{R}\right)^2 - \frac{5}{12}\left(\frac{\lambda}{mR}\right)^2 - \frac{1}{3}\frac{\ddot{R}}{R}(-3 + \lambda^2), \end{aligned}$$

$$a_{23} = 0, \quad b_{21} = 2Q - \lambda\frac{m}{R}, \quad b_{22} = 2\frac{\dot{R}}{R}, \quad b_{23} = 0,$$

$$a_{31} = 0, \quad a_{32} = 0,$$

$$\begin{aligned} a_{33} = & -\frac{1}{3}\dot{\lambda}^2 - \frac{1}{3}\kappa\Lambda - \frac{2}{3}Q^2 - \frac{1}{3}\kappa\rho - \frac{5}{3}\frac{\dot{R}}{R}\lambda\dot{\lambda} - \frac{1}{3}\ddot{\lambda}\lambda \\ & + \frac{2}{3}\frac{m}{R}\lambda Q - \frac{2}{3}\frac{\dot{R}^2}{R^2}\lambda^2 - \frac{1}{6}\lambda^2\frac{m^2}{R^2} - \frac{1}{3}\frac{\ddot{R}}{R}(-3 + \lambda^2), \end{aligned}$$

$$b_{31} = 0, \quad b_{32} = 0, \quad b_{33} = 2\frac{\dot{R}}{R},$$

$$d_1 = d_3 = 0,$$

$$\begin{aligned} d_2 = & R^2[-12\lambda\left(\frac{\dot{R}}{R}\right)^3 + \dot{\lambda}\frac{\dot{R}^2}{R^2}(-6 + 13\lambda^2) + 2\dot{\lambda}^3 + \lambda^2(\ddot{\lambda} + \lambda\frac{\ddot{R}}{R}) \\ & + \dot{\lambda}(4Q^2 + \kappa(2\Lambda - \rho) - 6\frac{m}{R}Q\lambda + \lambda(5\ddot{\lambda} + 2\lambda\frac{m^2}{R^2} + 9\lambda\frac{\ddot{R}}{R})) \\ & + \frac{\dot{R}}{R}(\ddot{\lambda}(3 + 7\lambda^2) + \lambda(17\dot{\lambda}^2 + 2\kappa\Lambda - 2Q^2 - \kappa\rho + \frac{m}{R}\lambda Q) \\ & + \lambda\frac{\ddot{R}}{R}(3 + 5\lambda^2))], \end{aligned}$$

$$\text{for } i \neq j: \quad a_{ij} = -a_{ji}, \quad b_{ij} = -b_{ji}.$$

The symmetric parts of Einstein-Cartan equations are given by:

$$(\hat{0}\hat{0}) : -2\lambda^2\frac{\ddot{R}}{R} + \frac{\dot{R}^2}{R^2}(3 - \lambda^2) + \frac{m^2}{4R^2}(-4 + 3\lambda^2) - 2\frac{\dot{R}}{R}\dot{\lambda}\lambda = \kappa(\rho + \Lambda) + \frac{2m\lambda Q}{R} - Q^2,$$

$$(\hat{1}\hat{1}) : 2(1 - \lambda^2)\frac{\ddot{R}}{R} + (1 - \lambda^2)\frac{\dot{R}^2}{R^2} - \frac{m^2\lambda^2}{4R^2} - \dot{\lambda}^2 - 5\frac{\dot{R}}{R}\dot{\lambda}\lambda - \ddot{\lambda}\lambda = \kappa\Lambda + Q^2 - \frac{m\lambda Q}{R},$$

$$(\hat{2}\hat{2}) : 2\frac{\ddot{R}}{R} + (1 - 3\lambda^2)\frac{\dot{R}^2}{R^2} - \frac{m^2\lambda^2}{4R^2} - 2\frac{\dot{R}}{R}\dot{\lambda}\lambda = \kappa\Lambda + Q^2 - \frac{m\lambda Q}{R},$$

$$\begin{aligned}
(\hat{3}\hat{3}) : (1 - \lambda^2)(2\frac{\ddot{R}}{R} + \frac{\dot{R}^2}{R^2}) - (4 - \lambda^2)\frac{m^2}{4R^2} - 5\frac{\dot{R}}{R}\dot{\lambda} - \dot{\lambda}^2 - \ddot{\lambda} &= \kappa\Lambda + Q^2, \\
(\hat{0}\hat{1}) : \frac{m\lambda}{R}(\lambda\frac{\dot{R}}{R} + \frac{3}{2}\dot{\lambda}) = \dot{Q}\lambda + 2\lambda Q + 3\lambda Q\frac{\dot{R}}{R}, \\
(\hat{0}\hat{2}) : 2\lambda(\frac{\dot{R}^2}{R^2} - \frac{\ddot{R}}{R}) &= 0, \\
(\hat{1}\hat{2}) : \frac{m}{2R}(\dot{\lambda} + 2\lambda\frac{\dot{R}}{R}) &= 0.
\end{aligned}$$

In the limit of small $\lambda^2 \ll 1$ we combine $\hat{0}\hat{0}$ and $\hat{1}\hat{1}$ components to approximate the time gradients of the cosmic scale factor:

$$\begin{aligned}
\frac{\dot{R}^2}{R^2} &= \frac{1}{3}(\kappa(\rho + \Lambda) - Q^2 + \frac{2m\lambda Q}{R} + (\frac{m}{R})^2), \\
\frac{\ddot{R}}{R} &= \frac{1}{2}(\frac{2}{3}\kappa\Lambda - \frac{1}{3}\kappa\rho + \frac{4}{3}Q^2 - \frac{5}{3}\frac{m\lambda Q}{R} - \frac{1}{3}(\frac{m}{R})^2).
\end{aligned} \tag{16}$$

The age of the Universe follows immediately:

$$\begin{aligned}
\tau_U(\text{Gyr}) &= \frac{10}{h} \int_{10^{-3}}^1 \frac{da}{a} [\Omega_\Lambda + \Omega_m a^{-3} - \frac{1}{3}Q^2 + \frac{2}{3}\frac{m\lambda Q}{a} + \frac{m^2}{3a^2}]^{-1/2}, \\
\lambda &= \lambda_0 a^{-1}, \quad Q = Q_0 a^{-3/2}; \quad m, \lambda_0, Q_0 \text{ evaluated in the unit } H_0 = 1.
\end{aligned} \tag{17}$$

Note that even a term linear in torsion Q is negative because [6] $m\lambda > 0 (m\lambda < 0)$ implies $Q < 0 (Q > 0)$.

The relation (3.31) of Ref. [32], as the equation of motion for the angular momentum of the Zel'dovich model, is no more valid.

Let us finally write the CDM spectrum used in numerical evaluations [8]:

$$\begin{aligned}
P(\mathbf{k}) &= |\delta_{\mathbf{k}}|^2 = \frac{Ak}{(1 + \beta k + \alpha k^{1.5} + \gamma k^2)^2}, \\
k &= |\mathbf{k}|, \quad \beta = 1.7(\Omega_m h^2)^{-1} \text{Mpc}, \quad \alpha = 9.0(\Omega_m h^2)^{-1.5} \text{Mpc}^{1.5}, \quad \gamma = 1.0(\Omega_m h^2)^{-2} \text{Mpc}^2.
\end{aligned} \tag{18}$$

5 Appendix B

One can introduce the following general vector variable fulfilling the Stewart-Walker lemma $\mathcal{D}_\mu(k) \equiv R^k(t)\rho^{-1}h_\mu^\nu \tilde{\nabla}_\nu \rho$. It is easy to verify that the correct Friedmann limes of density contrast can be achieved by rescaling the scalar invariant of the vector variable

$$\delta \propto R^{2-k}(t)[- \mathcal{D}_\mu(k)\mathcal{D}^\mu(k)]^{1/2}.$$

We show below that our choice ($k = 2$) and rescaled Ellis-Bruni choice ($k = 1$) [10] give different results for geometries beyond that of Friedmann. Thus, only our choice of the variable ($k = 2$) gives a correct density contrast without any ad hoc posterior rescaling.

Ellis-Bruni covariant vector variables are defined as [10]:

$$\begin{aligned}
\bar{\mathcal{D}}_\mu &\equiv R(t)\rho^{-1}h_\mu^\nu \tilde{\nabla}_\nu \rho, \\
\bar{\mathcal{L}}_\mu &\equiv R(t)h_\mu^\nu \tilde{\nabla}_\nu \Theta.
\end{aligned} \tag{19}$$

The same procedure as in Appendix A results in the following equation for a density contrast in the matter dominated epoch:

$$\begin{aligned}
& \ddot{\bar{D}}_\mu + a_\mu a^\lambda \bar{D}_\lambda + u_\mu a^\lambda \dot{\bar{D}}_\lambda + u_\mu a^\lambda \dot{\bar{D}}_\lambda - \frac{1}{2} \kappa \rho \bar{D}_\mu \\
& + (\dot{\bar{D}}_\lambda + \bar{D}_\nu (\sigma^\nu_\lambda + \tilde{\omega}^\nu_\lambda)) \left(\frac{2}{3} \Theta \delta_\mu^\lambda + u_\mu a^\lambda + \tilde{\omega}^\lambda_\mu + \sigma^\lambda_\mu \right) \\
& + \frac{2}{3} \Theta u_\mu a^\nu \bar{D}_\nu + \dot{\bar{D}}_\lambda (\tilde{\omega}^\lambda_\mu + \sigma^\lambda_\mu) + \bar{D}_\lambda (\dot{\sigma}^\lambda_\mu + \dot{\tilde{\omega}}^\lambda_\mu) \\
& - R [2a_\mu \dot{\Theta} + {}^{(3)}\tilde{\nabla}_\mu \mathcal{N} + \Theta a_\lambda \left(\frac{2}{3} \Theta \delta_\mu^\lambda + u_\mu a^\lambda + \tilde{\omega}^\lambda_\mu + \sigma^\lambda_\mu \right) \\
& \quad + \frac{1}{3} \Theta^2 a_\mu + \Theta a_\mu] = 0.
\end{aligned} \tag{20}$$

The corresponding equations in the local Lorentzian frame are:

$$\ddot{\bar{D}}_i + \bar{b}_{ij} \dot{\bar{D}}_j + \bar{a}_{ik} \bar{D}_k + \bar{d}_i = 0, \quad i, j, k = 1, 2, 3, \tag{21}$$

$$\begin{aligned}
\bar{a}_{11} &= 2 \frac{\dot{R}^2}{R^2} + \frac{\ddot{R}}{R} - Q^2 - \frac{1}{2} \kappa \rho + \frac{m}{R} \lambda Q - \left(\frac{\lambda m}{2R} \right)^2, \\
\bar{a}_{12} &= \frac{1}{2} \frac{m}{R} \dot{\lambda} - \frac{7}{4} \frac{\dot{R}}{R} Q + \frac{3}{2} \lambda \frac{m}{R} \frac{\dot{R}}{R}, \quad \bar{a}_{13} = 0, \\
\bar{b}_{11} &= 4 \frac{\dot{R}}{R}, \quad \bar{b}_{12} = -2Q + \lambda \frac{m}{R}, \quad \bar{b}_{13} = 0,
\end{aligned}$$

$$\begin{aligned}
\bar{a}_{21} &= -\frac{1}{2} \lambda \frac{m}{R} + \frac{7}{4} \frac{\dot{R}}{R} Q - \frac{3}{2} \lambda \frac{\dot{R}}{R} \frac{m}{R}, \\
\bar{a}_{22} &= \frac{\ddot{R}}{R} - \dot{\lambda}^2 - Q^2 - \frac{1}{2} \kappa \rho - 2\lambda \lambda \frac{\dot{R}}{R} \\
& + \frac{m}{R} Q \lambda - \left(\lambda \frac{m}{2R} \right)^2 - \left(\frac{\dot{R}}{R} \right)^2 (-2 + \lambda^2),
\end{aligned}$$

$$\bar{a}_{23} = 0, \quad \bar{b}_{21} = 2Q - \lambda \frac{m}{R}, \quad \bar{b}_{22} = 4 \frac{\dot{R}}{R}, \quad \bar{b}_{23} = 0,$$

$$\bar{a}_{31} = 0, \quad \bar{a}_{32} = 0, \quad \bar{a}_{33} = 2 \frac{\dot{R}^2}{R^2} + \frac{\ddot{R}}{R} - \frac{1}{2} \kappa \rho,$$

$$\bar{b}_{31} = 0, \quad \bar{b}_{32} = 0, \quad \bar{b}_{33} = 4 \frac{\dot{R}}{R},$$

$$\bar{d}_1 = \bar{d}_3 = 0,$$

$$\begin{aligned}
\bar{d}_2 &= R [2\dot{\lambda}^3 + \lambda^2 (\ddot{\lambda} + \frac{\ddot{R}}{R}) + \left(\frac{\dot{R}}{R} \right)^2 \dot{\lambda} (6 + 13\lambda^2) \\
& + \dot{\lambda} (4Q^2 + \kappa(2\Lambda - \rho)) - 6 \frac{m}{R} \lambda Q \\
& + \lambda (5\ddot{\lambda} + 2\lambda \frac{m^2}{R^2} + 9\lambda \frac{\ddot{R}}{R}) \\
& + \frac{\dot{R}}{R} (\dot{\lambda} (3 + 7\lambda^2) + \lambda (17\lambda^2 + 2\kappa\Lambda - 2Q^2 \\
& - \kappa\rho + \frac{m}{R} \lambda Q + \lambda \frac{\ddot{R}}{R} (3 + 5\lambda^2))],
\end{aligned}$$

$$\text{for } i \neq j : \bar{a}_{ij} = -\bar{a}_{ji}, \quad \bar{b}_{ij} = -\bar{b}_{ji}.$$

The authors in [10] equalize components of their variables \bar{D}_μ with a scalar density contrast δ . This is possible in the Friedmann limes when all components are equal. However even then, the scalar quantity formed from their variables must be ad hoc multiplied by the cosmic scale factor to achieve the correct result:

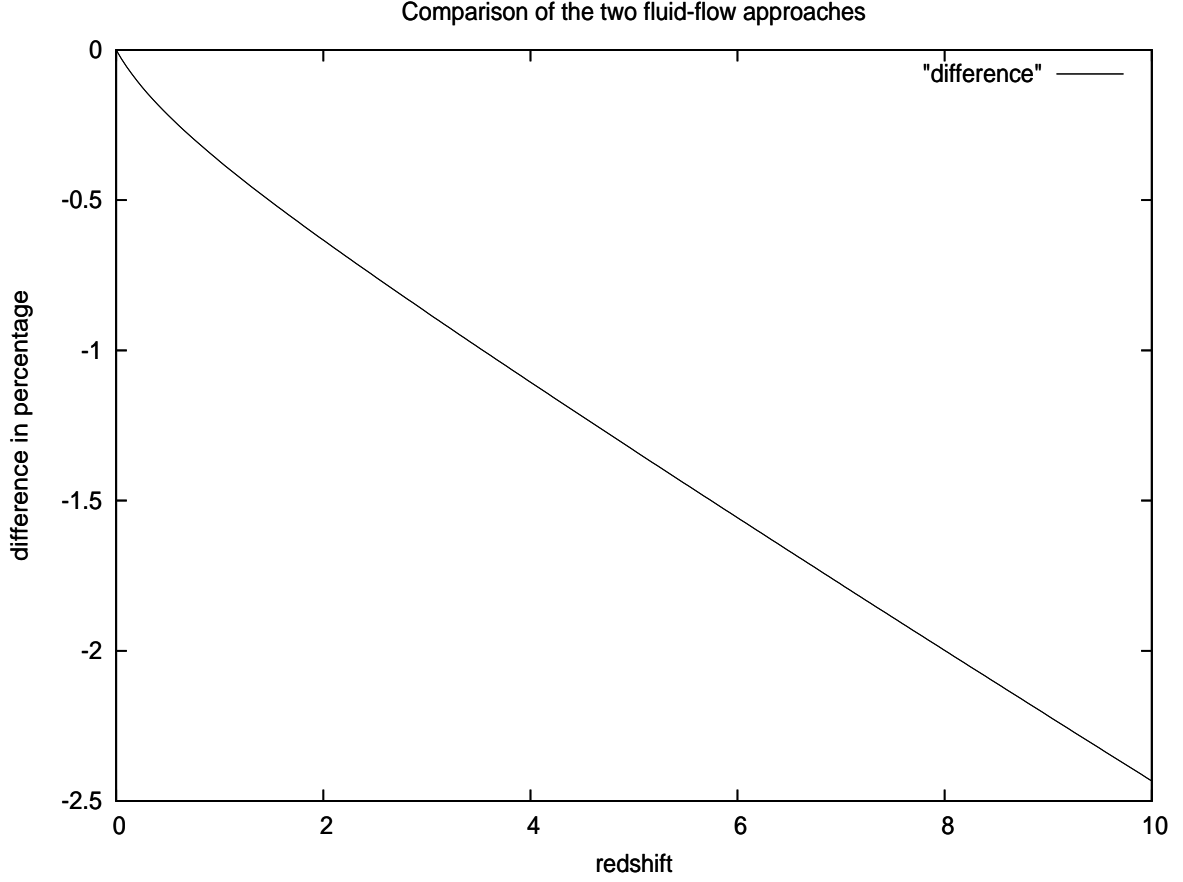


Fig. 4. Comparison between the two fluid-flow approaches for the model EC3: $\delta \equiv [-\mathcal{D}_\mu \mathcal{D}^\mu]^{1/2}$ and $\bar{\delta} \equiv R(t)[- \bar{\mathcal{D}}_\mu \bar{\mathcal{D}}^\mu]^{1/2}$, difference $\equiv (\delta - \bar{\delta})/\delta$, $\delta(z=0) = \bar{\delta}(z=0) = 1$.

$$\delta \propto R(t)[- \bar{\mathcal{D}}_\mu \bar{\mathcal{D}}^\mu]^{1/2}.$$

Our corrected variables \mathcal{D}_μ , on the contrary, give immediately good and correct Friedmann limes:

$$\delta \propto [-\mathcal{D}_\mu \mathcal{D}^\mu]^{1/2} = [-\mathcal{D}_a \mathcal{D}^a]^{1/2} \quad (22)$$

Let us stress that beyond Friedmannian geometry two quantities are not equal:

$$R(t)[- \bar{\mathcal{D}}_\mu \bar{\mathcal{D}}^\mu]^{1/2} \neq [-\mathcal{D}_\mu \mathcal{D}^\mu]^{1/2},$$

hence we use throughout our paper corrected variables \mathcal{D}_μ . In Fig. 4 the reader can find comparison between two formulas when the vorticity and the acceleration do not vanish.

References

1. D. Palle, Nuovo Cim. **A 109**, 1535 (1996)
2. D. Palle, Nuovo Cim. **B 115**, 445 (2000); ibidem **B 118**, 747 (2003)
3. F. Aharonian et al.(H.E.S.S. Collaboration), Phys. Rev. Lett. **97**, 221102 (2006)
4. D. P. Finkbeiner, Astrophys. J. **614**, 186 (2004)
5. D. Palle, Nuovo Cim. **B 111**, 671 (1996)
6. D. Palle, preprint **arXiv:0802.2060v2** (2009)

7. P. J. E. Peebles, *The Large-Scale Structure of the Universe*, (Princeton University Press, New Jersey 1980)
8. E. W. Kolb, M. S. Turner, *The Early Universe* (Addison-Wesley, Redwood City 1990)
9. T- Padmanabhan, *Structure formation in the Universe* (Cambridge University Press, Cambridge 1995)
10. G. F. R. Ellis, M. Bruni, Phys. Rev. **D 40**, 1804 (1989); G. F. R. Ellis, J. Hwang, M. Bruni, *ibidem* **D 40**, 1819 (1989); G. F. R. Ellis, M. Bruni, J. Hwang, *ibidem* **D 42**, 1035 (1990)
11. J. M. Stewart, M. Walker, Proc. R. Soc. Lond. **A 341**, 49 (1974)
12. M. J. Longo, preprint [arXiv:0812.3437](https://arxiv.org/abs/0812.3437) (2008)
13. A. Cooray, Phys. Rev. **D 65**, 103510 (2002)
14. A. Kashlinsky, F. Atrio-Barandela, D. Kocevski, H. Ebeling, *Astrophys. J.* **686**, L49 (2008); A. Kashlinsky, F. Atrio-Barandela, H. Ebeling, A. Edge, D. Kocevski, *Astrophys. J.* **712**, L81 (2010)
15. R. Watkins, H. A. Feldman, M. J. Hudson, *M.N.R.A.S.* **392**, 743 (2009); H. A. Feldman, R. Watkins, M. J. Hudson, *ibidem* **392**, 756 (2009)
16. G. Lavaux, R. B. Tully, R. Mohayaee, S. Colombi, *Astrophys. J.* **709**, 483 (2010)
17. K. Land, J. Magueijo, Phys. Rev. Lett. **95**, 071301 (2005)
18. M. R.olta et al. (WMAP Collaboration), *Astrophys. J. Suppl.* **180**, 296 (2009)
19. A. G. Riess et al., *Astrophys. J.* **699**, 539 (2009)
20. J. A. S. Lima, J. V. Cunha, J. S. Alcaniz, Phys. Rev. **D 68**, 023510 (2003); D. Rapetti, S. W. Allen, A. Mantz, *M.N.R.A.S.* **388**, 1265 (2008); A. Vikhlinin et al., *Astrophys. J.* **692**, 1060 (2009)
21. S. C. Vauclair et al., *Astron. and Astrophys.* **412**, L37 (2003); A. Blanchard, M. Douspis, M. Rowan-Robinson, S. Sarkar, *Astron. and Astrophys.* **449**, 925 (2006); L. D. Ferramacho, A. Blanchard, *Astron. and Astrophys.* **463**, 423 (2007)
22. H. Liu, T.-P. Li, preprint [arXiv:0907.2731](https://arxiv.org/abs/0907.2731) (2009); H. Liu, T.-P. Li, preprint [arXiv:1003.1073](https://arxiv.org/abs/1003.1073) (2010); B. F. Roukema, preprint [arXiv:1004.4506](https://arxiv.org/abs/1004.4506) (2010)
23. U. Sawangwit, T. Shanks, preprint [arXiv:1006.1270](https://arxiv.org/abs/1006.1270) (2010)
24. R. Kessler et al., *Astrophys. J. Suppl.* **185**, 32 (2009)
25. S. Basilakos, M. Plionis, J. A. S. Lima, preprint [arXiv:1006.3418](https://arxiv.org/abs/1006.3418) (2010)
26. P. Kroupa et al., preprint [arXiv:1006.1647](https://arxiv.org/abs/1006.1647) (2010), *Astron. and Astrophys.* in press
27. M. R. S. Hawkins, *M.N.R.A.S.* **405**, 1940 (2010)
28. S. Basilakos, J. C. Bueno Sanchez, L. Perivolaropoulos, Phys. Rev. **D 80**, 043530 (2009)
29. R. Bean, M. Tangmatitham, Phys. Rev. **D 81**, 083534 (2010)
30. F. Zwicky, *Helv. Phys. Acta* **6**, 110 (1933)
31. J. A. Schouten, *Ricci-Calculus* (Springer Verlag, Berlin 1954)
32. Yu. N. Obukhov, V. A. Korotky, *Class. Quantum Grav.* **4**, 1633 (1987)
33. Th. Chrobok, Yu. N. Obukhov, M. Scherfner, Phys. Rev. **D 63**, 104014 (2001)
34. Th. Chrobok, H. Herrmann, G. Rueckner, *Technische Mechanik* **22**, 1 (2002)
35. D. Palle, *Nuovo Cim.* **B 114**, 853 (1999)
36. S. D. Brechet, M. P. Hobson, A. N. Lasenby, *Class. Quant. Grav.* **24**, 6329 (2007)